UK Atomic Energy Authority

UKAEA-STEP-PR(23)03

William Iliffe, Kirk Adams, Nianhua Peng, Greg Brittles, Rod Bateman, Aidan Reilly, Chris Grovenor, Susannah Speller

The effect of in-situ irradiation on the superconducting performance of REBCO coated conductors

The effect of in-situ irradiation on the superconducting performance of REBCO coated conductors

William Iliffe, Kirk Adams, Nianhua Peng, Greg Brittles, Rod Bateman, Aidan Reilly, Chris Grovenor, Susannah Speller

This is a preprint of a paper submitted for publication in Materials Research Letter

The effect of in-situ irradiation on the superconducting performance of $REBa_2Cu_3O_{7-\delta}$ coated conductors

Will Iliffe[1,4], Kirk Adams[1], Nianhua Peng[2], Greg Brittles[3], Rod Bateman[3], Aidan Reilly[4], Chris Grovenor[1], Susannah Speller[1]

[1] Department of Materials, University of Oxford, Oxford OX1 3PH, United Kingdom
2 Surrey Ion Beam Centre, Surrey University, Guildford GU2 7XH, United Kingdom
3- Tokamak Energy, 173 Brook Dr, Milton, Abingdon OX14 4SD, United Kingdom
4- Culham Centre for Fusion Energy, Abingdon, OX14 3DB, United Kingdom

Abstract

Commercial fusion power plants will require strong magnetic fields that can only be achieved using state-of-the-art high temperature superconductors in the form of $REBa_2Cu_3O_{7-\delta}$ coated conductors. In operation in a fusion machine, the magnet windings will be exposed to fast neutrons that are known to adversely affect the superconducting properties of $REBa_2Cu_3O_{7-\delta}$ compounds. However, very little is known about how these materials will perform when they are irradiated at cryogenic temperatures. Here we use a bespoke in-situ test rig to show that helium ion irradiation produces a similar degradation in properties regardless of temperature, but room temperature annealing leads to substantial recovery in the properties of cold irradiated samples. We also report the first attempt at measuring the superconducting properties whilst the ion beam is incident on the sample, showing that the current that the superconductor can sustain is reduced by a factor of 3 when the beam is on.

1. Introduction

One option for the long term decarbonization of electricity generation is to utilize the energy released when atoms with low binding energy fuse. Research into nuclear fusion reactors was started in the 1950s, and continues at an increasing pace in both private companies [1]–[4] and national and international laboratories [5], [6]. Current fusion reactor demonstrators, most of which are based on the tokamak concept [7], use strong magnetic fields to confine plasmas of deuterium and tritium. Because the physical space for magnet windings is often extremely limited, these magnets require conductors that can transport very high current densities (J), making superconducting materials the only viable option. Coated conductors (CC) made with a biaxially textured layer of the anisotropic high temperature superconductor (HTS) $REBa_2Cu_3O_7$ (RE= rare-earth, REBCO) compounds are seen as a key enabling technology for small fusion reactors [8], [9] owing to their very large engineering critical current densities (J_e) in high magnetic fields and at temperatures well above 4.2 K. However, in service the electromagnets in a tokamak are exposed to fluxes of fast neutrons [10] even with the addition of shielding materials [11], [12], and it is known that the performance of superconducting materials degrades as a result of the damage created by neutron irradiation [13]–[15].

As with all type II superconductors, the critical current density (J_c) of the REBCO layer in a CC is determined by the flux pinning landscape[1], produced in part by microstructural defects, and is influenced by temperature (T), applied magnetic field vector (**B**) and strain (ε). As irradiation with energetic particles modifies the defect landscape [16], [17], J_c also evolves with fluence (ϕ) - number of incident particles per unit area - and depends on the particular type and energy of the irradiating particles. The resultant damage level in a given material is often reported in units of displacements

[1] The size, shape and distribution of defects relative to the characteristic penetration and coherence lengths of the superconducting material [49].

per lattice atom (dpa), as this unit has been shown to correlate well with macroscopic changes in material properties [18].

The extreme conditions experienced in the toroidal field (TF) magnet [19] in a tokamak make this a particularly challenging application for REBCO CCs, especially because of the smaller scale of the latest generation of tokamak reactors (eg. [1], [4], [6]). Designing these magnets for long term operation will require detailed information on how the superconducting performance of REBCO CC at the operating temperature is influenced by simultaneous irradiation with both fusion spectrum neutrons and gamma rays, ideally with the superconductor carrying its full rated current and subject to high applied fields and strain. Given that no source of DT fusion neutrons of the appropriate fluence currently exists, experiments to determine $J_c(\boldsymbol{B}, T, \varepsilon, \phi)$ values under true fusion conditions have not been possible. The majority of published experimental measurements have involved irradiating the CC samples at room temperature or above, followed by transferring them to a cryogenic measurement system to evaluate the effect of the irradiation on J_c as a function of temperature and applied magnetic field. Notable examples of this kind of ex-situ experiment include exposure of CC to fission spectrum neutrons by Fischer et al. [14], [20] and energetic ions (eg. [21], [22]). These experiments all showed a systematic decrease in both critical temperature (T_c) and J_c in low field, accompanied by a decrease in anisotropy. However, in higher applied fields, J_c values initially increase with irradiation damage, before decreasing with further irradiation until eventually there is a complete loss of superconductivity. The fluence at which the peak in J_c occurs has been shown to be dependent on the sample temperature, the type of radiation, the direction of the applied field and the nature of the original pinning landscape in the CC [20]. A more thorough description of these experiments can be found in [23].

More recently, steps towards testing REBCO CC under fusion relevant conditions, such as cryogenic temperatures, have been undertaken. The first such experiment was reported by Sorbom [24] who used 1.2 MeV protons to irradiate YBCO CCs up to ≈ 0.003 dpa (3 mdpa) at 80 K, 323 K and 423 K before allowing the samples to return to room temperature for an extended period prior to performing cryogenic transport measurements. Sorbom's key conclusions were that irradiating REBCO at a lower temperature led to a slower decline in J_c value with increasing fluence. It was inferred from supporting molecular dynamics (MD) simulations that a higher proportion of the radiation-induced lattice defects formed at lower temperatures remained as isolated point defects because the slower diffusion kinetics restricted migration to and accumulation at the numerous low angle grain boundaries present in these materials [24]. We have recently reported the first in-situ J_c measurements on CC samples at 40 K in self-field, taken in between sequential irradiation doses with 2 MeV He^+ ions without the samples being warmed to room temperature. By comparing the degradation in performance when the samples were both irradiated and measured in-situ at 40 K with samples irradiated at room temperature and then cooled for ex-situ measurement [23], [25] we showed that, even though the J_c of both sets of samples seemed to degrade at approximately the same rate with increasing fluence, the J_c and T_c values of the cold-irradiated samples could be recovered to some extent after 'annealing' at room temperature, whereas the superconducting properties of the room-temperature-irradiated samples declined slightly on further ageing at room temperature. Most recently, Fischer et al. used proton irradiation at 77 K to investigate how annealing at 80 – 300 K affected the J_c and T_c values of damaged REBCO CC samples. Their results showed that there was no change in I_c values up to 110 K, suggesting that the irradiation-induced damage in REBCO is stable up to this temperature, but even short exposures to temperatures above 110 K led to improvements in both J_c and T_c values [26]. In light of these new in-situ experiments, the apparent improvement in damage tolerance of CCs at low temperature reported in the original Sorbom study [24] can now be understood to result from the annealing out of some of the irradiation induced

defects during the room temperature excursion before the superconducting properties were measured. The recovery of CC properties upon room temperature annealing after cold irradiation, and the importance of establishing whether the life of fusion magnets can be extended by annealing, led Unterrainer et al. to study the effects of annealing samples after neutron irradiation in a fission reactor. They found that both T_c and J_c values recovered on annealing at temperatures up to 200°C, with further property recovery at higher annealing temperatures when an oxygen atmosphere was used [27].Even after this relatively small number of publications, it is already clear that irradiation with neutrons and ions creates lattice damage that results in a reduction in both the key superconducting parameters (T_c and J_c), and that the temperature history of the sample during and after irradiation is important in determining the superconducting properties and hence predicting the magnet performance under real service conditions.

The next step in emulating real operational conditions is to measure the superconducting properties while the lattice damage is being created – i.e. when neutrons or ion beam is interacting with the sample. Here we report new experiments in which a GdBCO CC sample is cooled below T_c and then exposed to He^+ ion irradiation while transporting a supercurrent. This has required a substantial re-design of our original experimental protocols. In addition, we have increased the number of cold and room temperature irradiated samples measured with the beam off, added measurements taken after much shorter room temperature anneals, and explored the effect of a sequence of cold irradiation damage and room temperature recovery cycles.

2. Experimental Set-up

The material used for this work was a GdBCO-based CC with a 2 µm thick superconducting layer manufactured by Fujikura in 2018 using a combination of ion beam assisted deposition and pulsed laser deposition [28], [29]. Full details of the experimental set-up are described in [23] and [25]. Briefly, in collaboration with the Surrey Ion Beam Centre (SIBC), an apparatus was built to measure the current-voltage (I-V) characteristics of 40-50 µm wide tracks prepared in CCs using wet etching and photolithography whilst the sample is maintained at 40 K and exposed to irradiation damage by 2 MeV He^+ ions. To minimize heating of the sample, transport measurements were taken using square current pulses of duration < 0.12 s, with intervals between the pulses of > 0.5 s. I-V curves were constructed by gradually increasing the amplitude of the current pulse and measuring the voltage during the duration of the pulse. The curves were fitted to a power law to determine I_c and n-values using:

$$V = E_c L \left(\frac{I}{I_c}\right)^n$$

where L is the track length and E_c is the electric field criterion. In line with other similar experiments (eg. [30], [31]), a criterion of E_c = 1 µV cm^{-1} was used to extract I_c values. Quenches that might damage the tracks were avoided by increasing the pulse amplitude by the smallest possible increment allowed by the power supply (0.02 A) and stopping the experiment when only a small voltage was measured across the superconducting track (V ≈ 30 µV). Here, T_c is defined as the temperature where the resistance of the sample is 50% of that measured at 100 K and the transition width (ΔT_c) is defined as the temperature range over which the sample resistance changes from 10% to 90 % of the 100 K resistance value. T_c measurements were performed with a constant current of ≈ 0.1 A (J≈0.1 MA cm^{-2}).

Since this study is aimed at mimicking neutron damage in REBCO, analysis using the SPECTRA-PKA code [32], [33] was used to define suitable irradiation parameters for our sample based on the neutron irradiation experiments of Fischer et al. [20]. In these experiments, a GdBCO CC was irradiated in the

Central Irradiation Facility of the Vienna TRIGA reactor [34] with fission spectrum neutrons up to a total fluence of ≈ $4x10^{18}$ n_f cm^{-2}, where n_f is the number of fast neutrons (defined as neutrons with energy > 0.1MeV). This is equivalent to a damage level of 4.4 mdpa accumulated at a rate of $8.3x10^{-9}$ dpa s^{-1}, and the SPECTRA-PKA calculation suggests that oxygen primary knock-ons contribute the largest proportion (59.2%) of the total damage [25]. SRIM[2] analysis [35] was then used to define a suitable ion-energy combination that would allow us to excite the oxygen ions in the REBCO lattice. Selecting a dpa rate similar to that achieved in the TRIGA reactor would occupy the SIBC beam line for unacceptably long periods, so a rastered beam of 2 MeV He^+ ions at a beam current density of 100 nA cm^{-2} was selected to provide a damage rate of $6.4x10^{-7}$ dpa s^{-1} (≈77 times faster than the TRIGA damage rate) and requiring an total cumulative irradiation duration of ≈ 130 minutes to reach damage levels similar to the maximum fluence reached by Fischer et al. (4.4 mdpa) [20].

Following the method described by Unterrainer et al. [27], a furnace annealing study on one of the cold irradiated samples (C4) was performed in flowing oxygen in a tube furnace. The sample was heated at 20 ^{0}C min^{-1} to 150 ^{0}C and held at this temperature for 24 hours, after which the sample was allowed to cool naturally inside the furnace.

The samples reported in this work were tested under two distinct conditions, referred to as "beam-on" and "beam-off", respectively. An additional protocol (see Figure 1) was developed for the beam-on experiments to protect the sample from thermal runaway in the event that the beam dramatically degraded the superconducting properties. The beam-on protocol involved increasing the magnitude of the current pulses in coarse steps (to minimize the time taken) to determine a rough beam-on I_c value at which the voltage exceeds the overvoltage limit (i.e. V > 30 μV). After a short delay of >60 s to allow the temperature equilibrium to re-establish, a series of repeated current pulses of constant magnitude below this initial beam-on I_c estimate were applied to the sample as irradiation progressed, and the stability of the voltage was monitored.

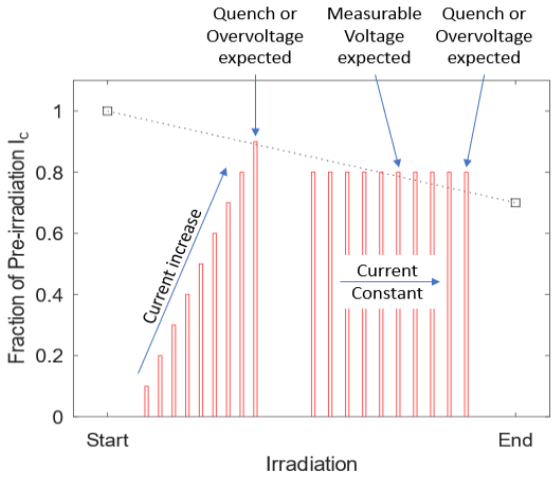

Figure 1: Schematic for beam-on testing protocol. The beam-off I_c is measured before and after ion irradiation (□) and the dotted line illustrates an extrapolation of how the I_c value might decrease gradually under irradiation. During the irradiation period, the current pulses are applied to the sample in 2 stages. Firstly the current is increased in coarse steps until an overvoltage response is detected. After a short delay to allow re-establishing of the temperature equilibrium, several current pulses of constant magnitude just under this peak current value are applied so that as the sample I_c degrades

[2] For parameters, see footnote 5 of [23].

under irradiation a voltage will be measured when the applied current exceeds this gradually decreasing I_c value.

3. Results

3.1 Beam-off experiments

Details of the superconducting properties of all the samples discussed in this work, including those for the 6 samples reported in [23], are shown in **Error! Reference source not found.**. These show that T_c > 90K – similar to the value determined using magnetometry – and ΔT_c < 2K for all samples except the anomalous sample RT2[3]. Scanning Electron Microscopy (SEM) was used to determine the actual width of each track and confirms that the new samples reported in this work are free from cracks at the track edges that were commonly seen in the original samples reported in [23] and can be attributed to extra care taken in the processing of the tracks (see supplementary figure S1).

Table 1: Pristine Sample Properties.

Track	Measured width [μm]	Length [mm]	T_c[K]	ΔT_c[K]	I_c(40K) ± 0.1	n(40K) ± 1	J_c(40K) [MA/cm^2]
C1	36	4	90.8	0.7	5.1	21	7.1
C2	38	4	90.2	1.3	12.3	24	16.2
C3	46	2	90.3	0.9	14.2	26	15.4
C4	46	2	90.5	0.9	14.1 [1]	30 [1]	15.3 [1]
C5	48	2	91.0	1.3	15.8	26	16.5
RT1	34	4	90.2	0.9	9.2	23	13.5
RT2	37	4	89.6	1.6	7.2	21	9.7
RT3	40	2	90.8	1.2	8.9	30	11.1
RT4	49	2	90.7	1.7	12.2	25	12.7
RT5	54	2	90.5	0.9	15.0	27	13.9
RT6	42	2	90.6	1.2	14.3	17	17.0

Notes:
[1] - only 1 I-V dataset collected as sample quenched and post quench the I_c had changed

Figure 2 illustrates the change of T_c, ΔT_c and the critical current density normalized to the unirradiated value for each sample (J_c/ J_c(initial)) measured at 40 K as a result of He^+ ion irradiation at room temperature (red) and in-situ at 40 K (blue). All three of these superconducting parameters degrade systematically with increased damage level, with the cold irradiated samples showing roughly the same damage rate as the room temperature irradiated samples. However, the samples that were irradiated cold show a significant increase in T_c and J_c/J_c(initial) and decrease in ΔT_c when allowed to anneal at room temperature for periods of ≈ 1 day, and then more gradually for much longer periods, whereas the properties of the samples irradiated at room temperature do not change significantly. This confirms our preliminary results reported in [23] and strongly supports our original conclusion that sample RT2 was anomalous. The time-dependent recovery of superconducting properties on holding at room temperature after cold irradiation is illustrated for samples C4 and C5 in Figure 3. This shows that, for both samples, there is a rather rapid increase in the T_c and I_c values as a result of room temperature annealing in the first 24 hours for sample C5, but that the recovery continues more slowly over much longer periods (≳ 150 days).

In addition, a cold irradiated and room temperature annealed sample (C4) has been subjected to a further cycle of in-situ irradiation and room temperature annealing (Figure 3a). To allow a direct

[3] Discussed in [23]

comparison with the room temperature annealing steps, the second cold irradiation experiment was stopped when the J_c/J_c(initial) value reached that obtained during the first cycle of cold irradiation (≈0.71 A). The results shown in Figure 2**Error! Reference source not found.** (and summarised in Supplementary Table 1) suggest that the J_c degradation in the second irradiation follows a similar trajectory as during the first cold irradiation, with T_c and ΔT_c returning to the same values that they had after the first cold irradiation. However, a key difference is that the rate of recovery of the superconducting properties after room temperature annealing is substantially slower after the second cold irradiation step, despite them being damaged to the same T_c, ΔT_c and J_c/J_c(initial) values prior to annealing. However, the sample cold irradiated twice does seem to eventually recover to a similar degree, with T_c and I_c(40 K) values increasing to ≈ 95% and 80 % of their pre-second cold irradiation values respectively (although this conclusion is based on only one datapoint). Finally, C4 was subjected to a furnace anneal at 150^{0}C in flowing oxygen for 24 hours. This led to further recovery of T_c, ΔT_c and I_c to values slightly higher than after the first room temperature anneal, as shown in Figure 3 and **Error! Reference source not found.**.

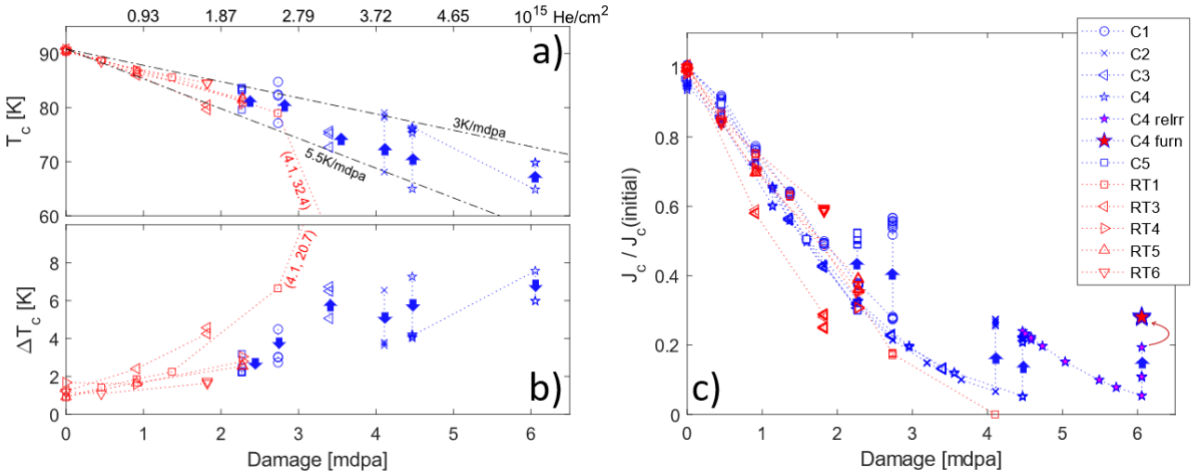

Figure 2: Evolution of the critical temperature T_c (a), the transition width ΔT_c (b) and the critical current density (J_c) relative to its initial, unirradiated value (J_c(initial)) at 40 K. Samples C1-5 were irradiated and measured in-situ at 40 K without a warming step, and samples RT1-6 were irradiated at room temperature and then cooled for measurement. Filled blue arrows indicate changes due to room temperature annealing. The top axis shows the cumulative fluence of 2MeV helium ions to the sample. Specific to sample C4 are 'relrr' which indicates data collected during and after a second cold irradiation step, and 'furn' which indicate data collected after furnace annealing at 150^{o}C.

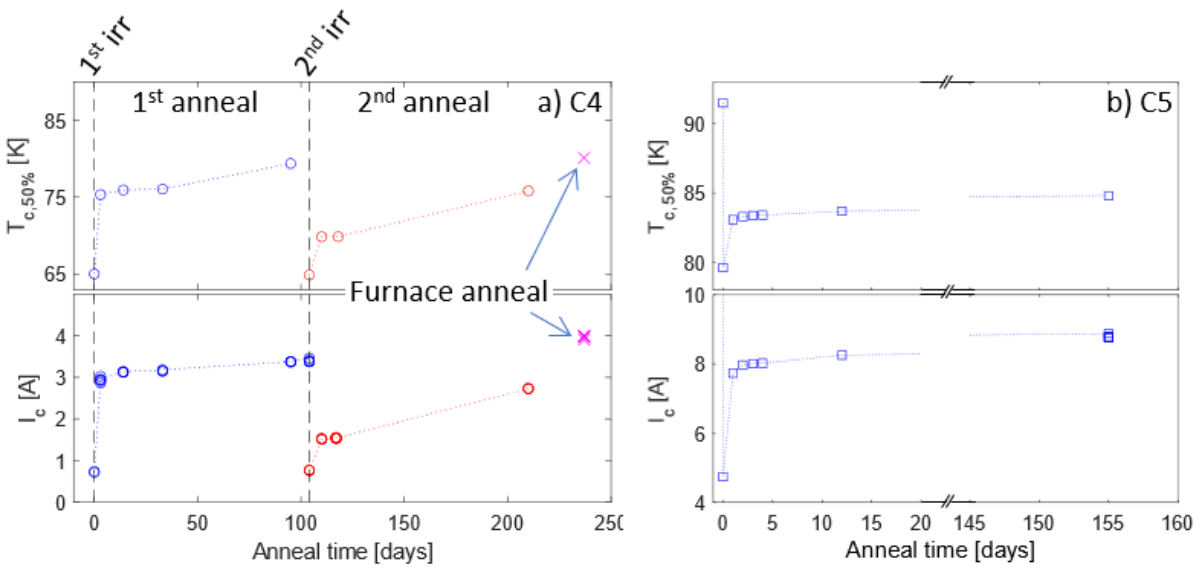

Figure 3: Evolution of the critical temperature ($T_{c,50\%}$) and critical current at 40 K (I_c) of cold-irradiated samples a) C4 and b) C5 on annealing at room temperature. Both $T_{c,50\%}$ and I_c values show an initial quick recovery over 1-2 days after cold irradiation followed by a further slower recovery over extended periods.

3.2 Beam-on experiments

Figure 4 shows the results of the beam-on experiments performed on sample C5 using the protocol shown in Figure 1. Beam-on tests were not performed during the first irradiation steps to ensure that this sample was reacting to the irradiation in a manner similar to previous in-situ irradiated samples, thus minimising the potential of blowing up the track. During the second irradiation step, the magnitude of the current pulse was increased to 6 A before an overvoltage (> 30 μV) was detected. The current pulse amplitude was then reduced to 5 A and maintained at that level for 13 consecutive 0.12 s pulses as the ion beam gradually added damage to the sample. Of these 13 pulses, 3 led to no measurable voltage response, 3 to a noisy voltage response (< 30 μV), 5 to an overvoltage (> 30 μV), and the final pulse led to a resistive quench (>> 30 μV). A beam-off measurement was then performed which confirmed that the sample had recovered from the quench, since the beam-off degradation of J_c followed the expected trend from the previous in-situ beam-off measurements. Further beam-on measurements were performed during subsequent irradiation stages. The maximum current that could be applied without a voltage being detected in the third irradiation stage was significantly lower than in the second irradiation stage (3 A compared to 5 A). Moreover, as the overall damage level increased during the third and fourth irradiation stages, pulses that led to voltage noise, over-voltages and resistive quenches became more common, even though the applied current was reduced.

As we became more familiar with the behaviour of the sample under ion beam irradiation, test conditions such as the pulse length and measurement frequency were varied to further probe the

sample performance. The results of a test of temperature and voltage stability under beam-on conditions – labelled #56 in Figure 4 - are shown in Supplementary Figure 2. This involved applying a 2.5 A, 100 s flat top pulse to the sample to assess whether the combination of rastering the beam and applying a continuous test current that was expected to elicit a voltage response affected the sample temperature and the nature of the voltage response. This test showed that the voltage across the superconductor was consistently noisy but < 30 µV, that the temperature of the sample did not rise significantly, and that the voltage response occasionally spiked during a period where current was applied for > 500 times longer than the normal current pulse used in the rest of the experiments, and 50 times longer than the rastering cycle period of the ion beam.

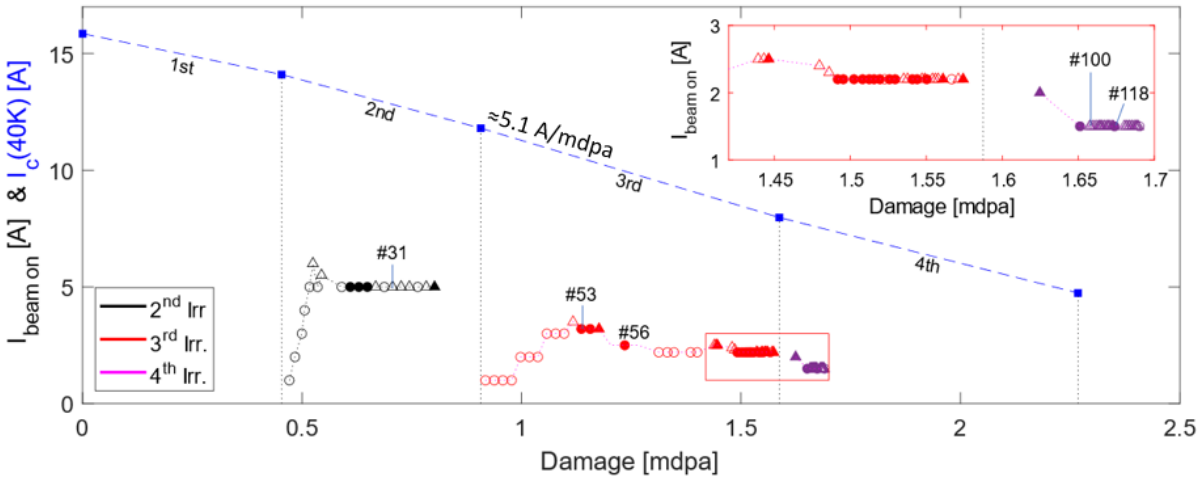

Figure 4: Current pulses applied to sample C5 during the 2nd (black), 3rd (red) and 4th (magenta) helium ion irradiation stages. Open circles (○): no measurable voltage response throughout current pulse. Filled circles (●): noisy voltage response during current pulse but did not exceed 30 µV. Open triangles (△): overvoltage detected. Filled triangles (▲): resistive quench of sample. Closed squares (■): I_c measurements whilst the beam was off. Numbered experiments refer to tests described in the supplementary information.

4. Discussion

4.1 Beam-off Experiments

The results of the beam-off experiments, summarised in **Error! Reference source not found.**, show that both the tracks previously reported (C1, C2 and RT1-4) and the new samples (C3-5 and RT5-6) have a spread of starting J_c values which can attributed to local variations in microstructure of the CC. However, the initial T_c and ΔT_c values for all the samples are > 89 K and < 1.7 K respectively, indicating that the REBCO layer is not significantly damaged by the track fabrication process. Further to the results reported in [23], the additional samples show a systematic decline in T_c at the rate of 5.5 K mdpa^{-1} and J_c/J_c(initial) at 25-45 % mdpa^{-1} for both cold and room temperature irradiation. This T_c declination rate is higher than the sample-independent rate reported Fischer et al. for irradiation with fission-spectrum neutrons (2.4 K mdpa^{-1}, [20]) and much higher than the 0.02-0.2 K mdpa^{-1} range inferred from data reported by Haberkorn et al. [36], Jia et al. [37] and Civale et al. [38] due to proton irradiation. The new in-situ samples showed a similar recovery in properties to the previously-reported samples on room temperature annealing, with measurements taken after shorter annealing times for sample C5 (Figure 3b) suggesting a rapid initial recovery of the superconducting properties

of these GdBCO tracks in the first days, followed by a gradual further recovery over much longer periods. Repeated in-situ irradiation and room temperature annealing of sample C4 (Figure 3a and in more detail in Supplementary Figure 4), shows that the damage and recovery process can be reproduced on the same sample.

Fischer et al. [26] have shown similar recovery behaviour at temperatures as low as 110 K in proton irradiated REBCO, which suggests at least one recovery mechanism must have a low activation energy (E_a). Unterrainer et al. [27] have also explored recovery in neutron irradiated samples at higher temperatures, showing that processes with much higher activation energies (only activated above 500 K) are also important in controlling T_c and J_c values if the loss of oxygen can be avoided. We have added our observation above that annealing a He^+ irradiated sample in oxygen to 420 K for 24 hours also recovers the J_c beyond the values achieved by long term annealing at 300 K.

There seems therefore to be a general consensus that cold irradiation, by protons or He^+ ions leads to the creation of types of point defects that are different than those generated by room temperature irradiation – some that have relatively high activation energies (E_a) for migration and hence remain essentially immobile at room temperature, but can be annealed out at higher temperatures, and others that have much lower activation energies and can be removed even at 110 K. Given that we would expect the concentrations of these defects to increase roughly linearly with irradiation fluence [18], [39], there should be a systematic build-up of both immobile and mobile defect concentrations during irradiation at 40 K, followed in our annealing experiments (at 300 K and 450 K) by a decrease in the concentration of the defects that are mobile at each temperature. We illustrate in Figure 5 how a population of irradiation-induced defects with a distribution of E_a values might respond to annealing, and lead to a J_c performance similar to that we report in Figure 3. We are not able to propose the exact nature of the immobile and mobile defects, nor to speculate on what kind of defects are more detrimental to the superconducting properties, but note that Tolpygo et al. [40] conclude that plane site defects are much more detrimental to T_c than chain site disorder and that Grey et al. [41] and others [42]–[44] show that oxygen within REBCO is most easily displaced by irradiation because of its lower mass and relatively lower threshold displacement energy than the other ionic species in the REBCO lattice. To understand this in more detail will require investigation using experimental and modelling techniques that can identify the type of point defects generated under different damage conditions.

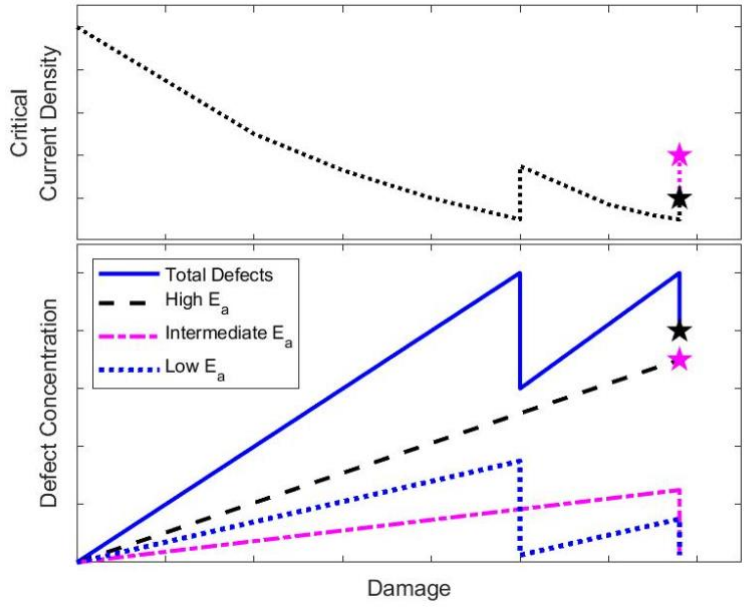

Figure 5: Schematic illustrating how a) critical current density and b) the populations of different types of defects – those immobile even at 420 K (high E_a--), immobile at 300 K but mobile at 420 K (intermediate E_a:) and those that become mobile at 300 K (low E_a-.) – could combine (-) to result in the recorded change in critical current density with increasing damage level and annealing of sample C4.

Since we are proposing that some of these specific defect populations can be reduced by annealing at room temperature, it is perhaps surprising that the rate of decline of J_c/J_c(initial) is similar for both in-situ samples irradiated and measured at 40 K and ex-situ samples irradiated at room temperature (Figure 2c). We speculate that this can be explained by dynamic annealing of the more mobile defects during room temperature irradiation to effectively reduce the damage rate. This seems to be confirmed by the observation that is no improvement in superconducting properties in the ex-situ samples after further room temperature annealing, noting that the time between irradiation and testing is typically several days. Therefore, we propose that the defect landscape created during irradiation is not the same at 300 K and 40 K, despite the apparent similarity in the rate of superconducting property degradation. It is possible during room temperature irradiation that defects mobile at this temperature do not simply diffuse to sinks or mutually annihilate during irradiation but that they combine into more stable defect clusters which can only then be removed at higher annealing temperatures. Further investigation of the microstructural differences between ex-situ irradiated and in-situ-post-annealed samples is therefore needed.

4.2 Beam-on Experiments

The results from the beam-on experiments (Figure 4) indicate that the superconducting performance of the REBCO tracks is substantially degraded under ion irradiation, which suggests that direct interactions with the energetic ions may adversely affect the superconducting state. However, we must first consider the possibility that, owing to insufficient cooling power, direct heating by the ion beam is gradually raising the temperature inside the REBCO layer and consequently reducing I_c. Preliminary tests on sample C5 suggest that the sample temperature would need to increase from 40 K to ≈ 65 K for the I_c to drop to ≈ 1/3 of its beam-off value whilst temperature sensor data shows deviations in temperature of less than ±1 K during the ion irradiation of this sample (see (Supplementary Figure 3). Even during the long pulse experiment (Supplementary Figure 2), application of the ion beam and a current of 2.5 A did not result in the temperature of the sample

rising by > 1 K, and the temperature control system acted sufficiently quickly to avoid any further temperature rise without reducing the heater output to zero. Although this gives us some confidence that there is no significant increase in temperature around the sample location during beam-on conditions, temperature increases in the narrow REBCO tracks cannot be completely ruled out as there is no temperature sensor in direct contact with the sample. However, a simple calculation based on modelling the REBCO layer as an isolated slab containing a random distribution of point heat sources with the surfaces of the slab held at a fixed temperature, the known flux of He^+ ions, the energy deposited in the REBCO layer per ion from SRIM calculations and the film thickness, suggest that the maximum temperature rise within the REBCO layer would be of the order of 10^{-4} K (for details, see supplementary information). We therefore conclude that the temperature rise in the sample during beam-on experiments is negligible compared to that required to reduce sample I_c to ≈ 1/3 of its beam-off value, and that it is some form of direct interaction with the ion beam that is affecting the superconducting properties of the track and reducing the current carrying capacity.

Energetic ions can interact and transfer energy to solid matter in two distinct processes: nuclear stopping and electronic stopping. In the nuclear stopping mechanism, energy is transferred from the incident ions to atoms in the material via elastic nuclear collisions. Provided the initial impact is sufficiently energetic, the target atom can be knocked out of its lattice site with enough energy to displace more atoms in the lattice, resulting in a small volume of material containing a concentration of point defects far above the equilibrium value [18]. If enough of these defects are formed locally, they may condense into a collision cascade where the crystal structure is lost, but there is no evidence that He^+ ions create this kind of gross damage [45]. The ballistic phase of the cascade, where atoms are being displaced, typically lasts for a fraction of a picosecond, and is followed by a slower relaxation process during which defects migrate and recombine, generally leaving some residual structural damage. Molecular dynamics simulations by Gray et al. [41] suggest that the defect structure in YBCO stabilizes within 1 ps, although any thermal effects are likely to take slightly longer to recover [44]. Presumably superconductivity would be disrupted locally within these regions, at least temporarily, even if there is minimal residual structural damage.

The electronic stopping mechanism involves charged incident beam ions undergoing a series of inelastic interactions with electrons, thereby losing energy gradually as they pass through the material. The subsequent thermalization of the highly excited electrons is expected to break numerous Cooper pairs, generating regions in the material where superconductivity is suppressed. If a transport current is present, it will redistribute to avoid these volumes, locally raising the current density. This mechanism is exploited in superconducting nanowire single photon detectors (SNSPD) [46] where a transport current is chosen so that, when an electron is excited by an incoming photon, the local current density either exceeds J_c temporarily or superconductivity is sufficiently suppressed to allow vortex movement within the track, generating a spike in voltage that can be detected [47].

To assess which of these mechanisms is more likely to be responsible for the observed degradation in I_c value of the tracks, we have carried out some simple calculations based on the irradiation conditions of our experiment. Since He^+ ions arriving at the REBCO surface are traveling at a velocity $v \approx 10^7$ m s^{-1} and at a flux $J = 6.25\text{x}10^{15}$ m^{-2} s^{-1}, the volume of sample containing one ion is $\frac{v}{J} \approx 1.6\text{x}10^{-9}$ m^3. This is several orders of magnitude larger than the track volume (~2 mm x 50 μm x 2 μm = 2.10^{-13} m^3) so we can assume that ions are travelling through the film one-by-one, even though we are using relatively high ion fluxes to accelerate the damage rate. Based on the total energy deposited in the REBCO layer per ion (calculated by SRIM to be $4.8\text{x}10^5$ eV) and the known flux of He^+ ions, we find that an energy of approximately 0.5 eV per unit cell per second is deposited into the REBCO layer. Over the course of a 120 ms measurement pulse, this equates to 60 meV per unit cell per pulse. This is

several orders of magnitude larger than the condensation energy of YBCO (≈0.2 meV) so it is reasonable to assume that there is sufficient energy deposited in the REBCO layer by electronic stopping of the He^+ ions during the measurement current pulse to severely disrupt the superconducting state. Moreover, the SRIM results suggest that these electronic interactions account for 99.9% of the energy deposited directly in the REBCO layer, making this a much more likely candidate than nuclear interactions to explain the weakening of superconducting state under irradiation with He^+ ions.

5. Conclusions

Here we report on further experiments investigating the recovery of the superconducting properties of biaxially textured GdBCO layers after 2MeV He^+ ion irradiation whilst the sample is maintained at 40 K, starting from both a pristine, unirradiated condition and after cold irradiation. Our results suggest that the defects created during cold irradiation have a range of activation energies, so that some can be annealed out – leading to the recovery of the superconducting properties – at temperature below 300 K for defects, others at 300-420 K, and a final group with higher activation energy that remain even after annealing at 420 K. This concept gives a clear focus for future modelling experiments to identify the nature of these defects so that the community can consider how to maximise the potential for recovery stages to reverse the degradation of superconducting properties after irradiation.

Using our new beam-on experimental protocol, we report that the voltage responses characteristic of the onset of instabilities and quenches are detected in CC tracks at much lower current densities during irradiation with 2 MeV He+ ions than the I_c values measured both before the ion beam is switched on and after it is turned off. After careful consideration of the possibility of this being a result of beam and/or ohmic heating effects, we conclude that this is a result of direct interactions between the energetic charged particle beam and the superconducting charge carriers. This interaction leads to a destabilisation of the superconducting state, specifically by the release of energy from the ion beam to the REBCO layer by electronic stopping, and that this results in the breaking of large number of Cooper pairs per incident ion.

The in-service conditions of magnets components in a fusion machine will involve primary collisions with energetic neutrons rather than light ions, and in the absence of Coulombic interactions we might expect no similar degradation effect. However, neutrons do generate both collision cascades and more widespread general lattice damage in REBCO [17], and so the primary knock-on ions generated from ballistic collisions with incident neutrons can then act like the He^+ ions as the source of electronic stopping damage that will degrade the superconducting properties. The flux of neutrons in magnet components will be much lower than the accelerated conditions we have used here, but we note that each incident neutron will be able to generate thousands of primary and secondary knock-on ions[4]. We further suggest that the preliminary in-situ experiments reported here indicate that the effect of irradiation damage on the performance of magnet windings will be impossible to avoid completely under fusion operation conditions, and so must be taken seriously in the design of superconducting electromagnets for fusion applications.

On behalf of all authors, the corresponding author states that there is no conflict of interest.
The datasets generated during and/or analysed during the current study are available from the corresponding author on reasonable request.

[4] Based on a 70keV oxygen PKA which was shown in [25] to be the primary knock-on atom-energy combination which was most prolific at generating lattice displacements in REBCO subject to 2 TF neutron spectra with vastly different neutron shielding philosophies.

References

[1] "Tokamak Energy Home Page," May 27, 2022. https://www.tokamakenergy.co.uk/ (accessed May 27, 2022).

[2] S. Reed, "Nuclear Fusion Edges Toward the Mainstream," *The New York Times*, Oct. 18, 2021.

[3] "Commenwealth Fusion Systems Home Page," May 27, 2022. https://www.cfs.energy/ (accessed May 27, 2022).

[4] B. N. Sorbom *et al.*, "ARC: A compact, high-field, fusion nuclear science facility and demonstration power plant with demountable magnets," *Fusion Engineering and Design*, vol. 100, pp. 378–405, Nov. 2015, doi: 10.1016/j.fusengdes.2015.07.008.

[5] M. Shimada *et al.*, "Chapter 1: Overview and summary," *Nuclear Fusion*, vol. 47, no. 6, Jun. 2007, doi: 10.1088/0029-5515/47/6/S01.

[6] "Spherical Tokamak for Energy Production UKAEA Home Page," May 27, 2022. https://step.ukaea.uk/ (accessed May 27, 2022).

[7] L. A. Artsimovich, "Tokamak devices," *Nuclear Fusion*, vol. 12, pp. 215–252, 1972, Accessed: May 27, 2022. [Online]. Available: http://iopscience.iop.org/0029-5515/12/2/012

[8] Y. Zhai, D. van der Laan, P. Connolly, and C. Kessel, "Conceptual design of HTS magnets for fusion nuclear science facility," *Fusion Engineering and Design*, vol. 168, Jul. 2021, doi: 10.1016/j.fusengdes.2021.112611.

[9] F. Dahlgren, T. Brown, P. Heitzenroeder, and L. Bromberg, "ARIES-AT magnet systems," *Fusion Engineering and Design*, vol. 80, no. 1–4, pp. 139–160, Jan. 2006, doi: 10.1016/j.fusengdes.2005.06.357.

[10] J. Freidberg, *Plasma Physics and Fusion Energy*, 1st ed., vol. 1. Cambridge: Cambridge University Press, 2007.

[11] A. Sykes *et al.*, "Compact fusion energy based on the spherical tokamak," *Nuclear Fusion*, vol. 58, no. 1, Jan. 2018, doi: 10.1088/1741-4326/aa8c8d.

[12] M. Coleman and S. McIntosh, "BLUEPRINT: A novel approach to fusion reactor design," *Fusion Engineering and Design*, vol. 139, pp. 26–38, Feb. 2019, doi: 10.1016/j.fusengdes.2018.12.036.

[13] M. Soell, C. A. M. van der Klein, H. Bauer Giesen, and W.-G. G. Vogl, "The influence of low temperature neutron irradiation on superconducting magnet systems for fusionreactors," *IEEE Transactions of Magnetics*, vol. MAG-11, no. 2, pp. 178–181, Mar. 1975.

[14] R. Prokopec, D. X. Fischer, H. W. Weber, and M. Eisterer, "Suitability of coated conductors for fusion magnets in view of their radiation response," *Superconductor Science and Technology*, vol. 28, no. 1, Jan. 2015, doi: 10.1088/0953-2048/28/1/014005.

[15] H. W. Weber, F. Nardai, C. Schwinghammer, and R. K. Maix, "Neutron Irradiation of NbTi with Different Flux Pinning Structures," in *Advances in Cryogenic Engineering Materials*, Boston, MA: Springer US, 1982, pp. 329–335. doi: 10.1007/978-1-4613-3542-9_32.

[16] K. Nordlund *et al.*, “Improving atomic displacement and replacement calculations with physically realistic damage models,” *Nature Communications*, vol. 9, no. 1, Dec. 2018, doi: 10.1038/s41467-018-03415-5.

[17] Y. Linden *et al.*, “Analysing neutron radiation damage in YBCO high-temperature superconuducting tapes,” *Journal of Microscopy*, pp. 1–10, 2021.

[18] G. Was, *Fundamentals of Radiation Materials Science*, 1st ed. Berlin, Heidelberg: Springer Berlin Heidelberg, 2007. doi: 10.1007/978-3-540-49472-0.

[19] M. R. Gilbert, T. Eade, C. Bachmann, U. Fischer, and N. P. Taylor, “Activation, decay heat, and waste classification studies of the European DEMO concept,” *Nuclear Fusion*, vol. 57, no. 4, Mar. 2017, doi: 10.1088/1741-4326/aa5bd7.

[20] D. X. Fischer, R. Prokopec, J. Emhofer, and M. Eisterer, “The effect of fast neutron irradiation on the superconducting properties of REBCO coated conductors with and without artificial pinning centers,” *Superconductor Science and Technology*, vol. 31, no. 4, Mar. 2018, doi: 10.1088/1361-6668/aaadf2.

[21] H. Matsui *et al.*, “Enhancement of critical current density in YBa2Cu3O7 films using a semiconductor ion implanter,” *Journal of Applied Physics*, vol. 117, no. 4, Jan. 2015, doi: 10.1063/1.4906782.

[22] N. Haberkorn, J. Guimpel, S. Suárez, J. H. Lee, H. Lee, and S. H. Moon, “Competition between pinning produced by extrinsic random point disorder and superconducting thermal fluctuations in oxygen-deficient GdBa2Cu3Ox coated conductors,” *Superconductor Science and Technology*, vol. 32, no. 12, Nov. 2019, doi: 10.1088/1361-6668/ab5164.

[23] W. Iliffe *et al.*, “In-situ measurements of the effect of radiation damage on the superconducting properties of coated conductors,” *Superconductor Science and Technology*, vol. 34, no. 9, Sep. 2021, doi: 10.1088/1361-6668/ac1523.

[24] B. N. Sorbom, “The Effect of Irradiation Temperature on REBCO J, Degradation and Implications for Fusion Magnets,” PhD Thesis, Massachuseets Institute of Technology, Cambridge, 2017. Accessed: May 30, 2022. [Online]. Available: https://dspace.mit.edu/handle/1721.1/120392?show=full

[25] W. Iliffe, “Radiation Damage of Superconducting Materials for Fusion Application,” DPhil Thesis, University of Oxford, Oxford, 2022. Accessed: May 30, 2022. [Online]. Available: https://ora.ox.ac.uk/objects/uuid:bab009f2-2b1d-42d7-a53c-bf914a128d7a

[26] D. Fischer, “Presentation: Degradation and annealing of coated conductors after cryogenic irradiation,” EUCAS Moscow, 2021.

[27] R. Unterrainer, D. X. Fischer, A. Lorenz, and M. Eisterer, “Recovering the performance of irradiated high-Temperature superconductors for use in fusion magnets,” *Superconductor Science and Technology*, vol. 35, no. 4, Apr. 2022, doi: 10.1088/1361-6668/ac4636.

[28] Fujikura Europe Ltd, “Fujikura HTS homepage.”

[29] S. Fujita *et al.*, “Flux-pinning properties of BaHfO 3 -doped EuBCO-coated conductors fabricated by Hot-Wall PLD,” *IEEE Transactions on Applied Superconductivity*, vol. 29, no. 5, 2019, doi: 10.1109/TASC.2019.2896535.

[30] S. C. Wimbush and N. M. Strickland, “A Public Database of High-Temperature Superconductor Critical Current Data,” *IEEE Transactions on Applied Superconductivity*, vol. 27, no. 4, Jun. 2017, doi: 10.1109/TASC.2016.2628700.

[31] N. M. Strickland, C. Hoffmann, and S. C. Wimbush, “A 1 kA-class cryogen-free critical current characterization system for superconducting coated conductors,” *Review of Scientific Instruments*, vol. 85, no. 11, Nov. 2014, doi: 10.1063/1.4902139.

[32] M. R. Gilbert and J. C. Sublet, “Differential dpa calculations with SPECTRA-PKA,” *Journal of Nuclear Materials*, vol. 504, pp. 101–108, Jun. 2018, doi: 10.1016/j.jnucmat.2018.03.032.

[33] M. R. Gilbert, J. Marian, and J. C. Sublet, “Energy spectra of primary knock-on atoms under neutron irradiation,” *Journal of Nuclear Materials*, vol. 467, pp. 121–134, Dec. 2015, doi: 10.1016/j.jnucmat.2015.09.023.

[34] H. W. Weber, H. Bock, E. Unfried, and L. R. Greenwood, “Neutron Dosimetry and Damage Calculations for the TRIGA Mark-II reactor in Vienna,” *Journal of Nuclear Materials*, vol. 137, pp. 236–240, 1986.

[35] J. F. Ziegler, J. P. Biersack, and M. D. Ziegler, *SRIM-Stopping Range of Ions in Matter*, 5th ed. Morrisvile: SRIM Company, 2015.

[36] N. Haberkorn, J. Kim, S. Suárez, J. H. Lee, and S. H. Moon, “Influence of random point defects introduced by proton irradiation on the flux creep rates and magnetic field dependence of the critical current density J c of co-evaporated GdBa2Cu3O7-δ coated conductors,” *Superconductor Science and Technology*, vol. 28, no. 12, Oct. 2015, doi: 10.1088/0953-2048/28/12/125007.

[37] Y. Chen, F. Yan, C. You, G. Zhao, and Y. Jiao, “Ultrafine nanocrystal precursor induced Jc increase of YBa 2Cu3O7-x films prepared using advanced low-fluorine solution,” *Journal of Alloys and Compounds*, vol. 576, pp. 265–270, 2013, doi: 10.1016/j.jallcom.2013.04.160.

[38] L. Civale *et al.*, “Defect Independence of the Irreversibility Line in Proton-Irradiated Y-Ba-Cu-0 Crystals,” *Physical Review Letters*, vol. 65, no. 9, pp. 1164–1167, 1990.

[39] M. T. Robinson, “Basic physics of radiation damage production,” 1994.

[40] S. K. Tolpygo, J.-Y. Lin, M. Gurvitch, S. Y. Hou, and J. M. Phillips, “Effect of oxygen defects on transport properties and Tc of YBCO: Displacement energy for plane and chain oxygen and implications for irradiation-induced resistivity and T c suppression,” *Physical Review B*, vol. 53, no. 18, pp. 462–474, 1996.

[41] R. L. Gray, M. J. D. Rushton, and S. T. Murphy, “Molecular dynamics simulations of radiation damage in YBa2Cu3O7,” *Superconductor Science and Technology*, vol. 35, no. 3, Mar. 2022, doi: 10.1088/1361-6668/ac47dc.

[42] F. Cui, H. Li, L. Jin, and Y. Li, “Simulations on radiation damage initiated by O(1) PKA in YBCO,” *Nuclear Instruments and Methods in Physics Research B*, vol. 91, pp. 374–377, 1994.

[43] F. Z. Cui, J. Xie, and H. D. Li, “Preferential radiation damage of the oxygen sublattice in YBa2Cu307.. A molecular-dynamics simulation,” *PHYSICAL REVIEW B*, vol. 46, no. 17, pp. 182–185, 1992.

[44] A. v. Krasheninnikov and K. Nordlund, “Ion and electron irradiation-induced effects in nanostructured materials,” *Journal of Applied Physics*, vol. 107, no. 7, p. 071301, Apr. 2010, doi: 10.1063/1.3318261.

[45] R. W. Harrison, N. Peng, R. P. Webb, J. A. Hinks, and S. E. Donnelly, “Characterisation of helium ion irradiated bulk tungsten: A comparison with the in-situ TEM technique,” *Fusion Engineering and Design*, vol. 138, pp. 210–216, Jan. 2019, doi: 10.1016/j.fusengdes.2018.11.024.

[46] L. You, “Superconducting nanowire single-photon detectors for quantum information,” *Nanophotonics*, vol. 9, no. 9, pp. 2673–2692, Sep. 2020, doi: 10.1515/nanoph-2020-0186.

[47] A. Engel, J. J. Renema, K. Il’In, and A. Semenov, “Detection mechanism of superconducting nanowire single-photon detectors,” *Superconductor Science and Technology*, vol. 28, no. 11, Sep. 2015, doi: 10.1088/0953-2048/28/11/114003.

[48] B. M. Terzijska, R. Wawryk, D. A. Dimitrov, C. Marucha, V. T. Kovachev, and J. Rafalowicz, “Thermal conductivity of YBCO and thermal conductance at YBCO/ruby boundary Part 1: joint experimental set-up for simultaneous measurements and experimental study in the temperature range 10-260 K.”

[49] T. Matsushita, *Flux Pinning in Superconductors*, 2nd ed., vol. 1. Springer, 2016.